Since January 2020 Elsevier has created a COVID-19 resource centre with free information in English and Mandarin on the novel coronavirus COVID-19. The COVID-19 resource centre is hosted on Elsevier Connect, the company's public news and information website.

Virology 513 (2018) 75–84

Contents lists available at ScienceDirect

Virology

journal homepage: www.elsevier.com/locate/virology

Coronavirus infectious bronchitis virus non-structural proteins 8 and 12 form stable complex independent of the non-translated regions of viral RNA and other viral proteins

Yong Wah Tan[a,b,c,1], To Sing Fung[a,1], Hongyuan Shen[c], Mei Huang[b], Ding Xiang Liu[a,*]

[a] South China Agricultural University, Guangdong Province Key Laboratory Microbial Signals & Disease Co, and Integrative Microbiology Research Centre, Guangzhou 510642, Guangdong, People's Republic of China
[b] School of Biological Sciences, Nanyang Technological University, 60 Nanyang Drive, 63755, Singapore
[c] Institute of Molecular and Cell Biology, 61 Biopolis Drive, Proteos 138673, Singapore

ARTICLE INFO

Keywords:
Coronavirus
Infectious bronchitis virus
IBV
Non-structure protein
RNA-dependent RNA polymerase
Protein interaction
RNA synthesis
Viral genome replication

ABSTRACT

The cleavage products from coronavirus polyproteins, known as the non-structural proteins (nsps), are believed to make up the major components of the viral replication/transcription complex. In this study, several nsps encoded by avian gammacoronavirus infectious bronchitis virus (IBV) were screened for RNA-binding activity and interaction with its RNA-dependent RNA polymerase, nsp12. Nsp2, nsp5, nsp8, nsp9 and nsp10 were found to bind to untranslated regions (UTRs), while nsp8 was confirmed to interact with nsp12. Nsp8 has been reported to interact with nsp7 and functions as a primase synthesizing RNA primers for nsp12. Further characterization revealed that nsp8-nsp12 interaction is independent of the UTRs of viral RNA, and nsp8 interacts with both the N- and C-terminal regions of nsp12. These results have prompted a proposal of how the nsp7-nsp8 complex could possibly function in tandem with nsp12, forming a highly efficient complex that could synthesize both the RNA primer and viral RNA during coronavirus infection.

1. Introduction

Coronaviruses are a family of enveloped viruses with single stranded, positive sense RNA genome of 27–30 kb in length. Infectious bronchitis virus (IBV) is an avian gammacoronavirus that causes respiratory disease in chickens, resulting in major economic burden to the poultry industry worldwide. In IBV-infected cells, a 3′-coterminal nested set of six mRNA species, including the genome-length mRNA (mRNA1) and five subgenomic mRNA species (mRNA2-6), is expressed. Four structural proteins, the type 1 glycoprotein spike (S), the small membrane-associated envelope protein (E), the integral membrane protein (M) and the phosphorylated nucleocapsid protein (N), are encoded by subgenomic mRNA (sgRNA) 2, 3, 4 and 6, respectively (Liu et al., 1991; Liu and Inglis, 1992a; Zhao et al., 1993). In addition, four accessory proteins, 3a, 3b, 5a and 5b are encoded by sgRNA 3 and 5 (Liu and Inglis, 1992a, 1992b).

During coronavirus infection, full-length genome is replicated for packaging into progeny virions, while sgRNAs are transcribed for the expression of structural proteins. These two processes are dependent upon viral ability to synthesize both the positive-sense genomic mRNA (gRNA) and a nested set of positive-sense sgRNAs. The key player in this part of the coronavirus life cycle is the virus-encoded replicase gene, which makes up two thirds of the genome and is translated into two polyproteins: pp1a and pp1ab. The two polyproteins are then auto-proteolytically processed into 16 non-structural proteins (nsps) by two virus-encoded proteases, the papain-like protease encoded in nsp3 and the 3C-like (main) protease encoded in nsp5 (Liu et al., 1994, 1995, 1997, 1998; Liu and Brown, 1995; Ng and Liu, 1998, 2000, 2002; Lim and Liu, 1998; Lim et al., 2000; Xu et al., 2001; Fang et al., 2008; Chen et al., 2009). Notably, due to the lack of a cleavage site that usually lies between nsp1 and nsp2 in other coronaviruses, cleavage of the IBV replicase only produces 15 nsps (nsp2-16) without the counterpart of nsp1. Based on sequence comparison, biochemical and structural studies, the enzymatic activities required for most of the key processes in coronavirus RNA synthesis have been mapped to some of the nsps (Pasternak et al., 2006). Among them, the key enzyme critical to the viral ability to replicate its genome and propagate in the host cell is the RNA-dependent RNA polymerase (RdRP) or nsp12. Available evidence suggests that the RNA polymerase activity of nsp12 may be primer-dependent (te Velthuis et al., 2010) and require the primase activity of

* Corresponding author.
E-mail address: dxliu0001@163.com (D.X. Liu).
[1] Equal contribution.

http://dx.doi.org/10.1016/j.virol.2017.10.004
Received 28 July 2017; Received in revised form 27 September 2017; Accepted 2 October 2017
Available online 13 October 2017
0042-6822/

nsp8 (Imbert et al., 2006). Other important enzymatic activities include the RNA helicase of nsp13 (Seybert et al., 2000; Ivanov et al., 2004a), the methyltransferase activities of nsp14 and nsp16 (Y. Chen et al., 2009; Ma et al., 2015; Decroly et al., 2008; Chen et al., 2011; Bouvet et al., 2010), the exoribonuclease activity of nsp14 (Ma et al., 2015; Minskaia et al., 2006) and the endoribonuclease activity of nsp15 (Ivanov et al., 2004b; Bhardwaj et al., 2004; Ricagno et al., 2006).

Information on the specific interactions among nsps is also emerging based on biochemical, structural and functional studies of nsps from other coronaviruses (Imbert et al., 2006; Ma et al., 2015; Imbert et al., 2008; von Brunn et al., 2007; Pan et al., 2008; Brockway et al., 2003; Subissi et al., 2014; Knoops et al., 2008). Distinct from the viral structural proteins, the functions served by the nsps are focused on the modulation of host environment to support viral replication and viral RNA synthesis. Integral membrane proteins nsp3, nsp4 and nsp6 engage in homotypic and heterotypic interactions to drive membrane rearrangements to form the network of double membrane vesicles (DMVs) and convoluted membranes (CMs) (Angelini et al., 2013), or double membrane spherules from zippered ER membranes (Maier et al., 2013), the sites of viral replication and also serve as the docking site for viral replication complexes (Oostra et al., 2008). A recent study has identified critical residues on nsp7 and nsp8 of severe acute respiratory syndrome coronavirus (SARS-CoV), which are essential for efficient *de novo* RNA synthesis by nsp12, indicating that interactions among these proteins contribute to the processivity of RNA synthesis (Subissi et al., 2014).

On the other hand, interaction between the nsps and viral RNA genome has not been thoroughly studied. Viral protein-RNA interactions are assumed to occur between the key replication enzymes, nsp7, nsp8 and nsp12, thus forming a complex exhibiting replicase activity in the presence of a RNA primer (Subissi et al., 2014). In addition, although some nsps have not been assigned with functions involved in coronavirus RNA synthesis, they might still be participating in viral RNA replication or transcription. In this study, a two-pronged approach was adopted to study viral proteins and protein-RNA interactions in coronavirus RNA synthesis. To elucidate RNA-protein interactions, an attempt was made to detect the presence of RNA-binding activity in any of the IBV nsps, which had not been previously reported to possess such an activity. This was done using available constructs over-expressing individual nsps in a biotin pull-down assay with biotinylated probes. The second method used was to conduct a screen for protein-protein interactions between viral polymerase, nsp12 and other nsps.

2. Material and method

2.1. Antibodies, enzymes and other reagents

Antibodies to β-tubulin, FLAG and HA tags were purchased from Sigma-Aldrich (St. Louis, MO, USA). Antisera against IBV proteins were made by immunization of rabbits with bacterially expressed fusion proteins as previously described (Liu et al., 1991; Fang et al., 2005). All horseradish peroxidase (HRP) conjugated secondary antibodies were purchased from Dako (Glostrup, Denmark) and Alexa Fluor® conjugated secondary antibodies were purchased from Invitrogen Molecular Probes® (Eugene, OR, USA). T7 RNA polymerase and Biotin RNA Labeling Mix were purchased from Roche Applied Science (Penzberg, Upper Bavaria, Germany). *Taq* polymerase and KOD Hot Start DNA Polymerase were purchased from KAPA Biosystems (Cambridge, MA, USA) and Merck (Darmstadt, Germany), respectively.

RPMI 1640 medium and Dulbecco's Modified Eagle Medium (DMEM) were purchased from Invitrogen (Carlsbad, CA, USA). Fetal Bovine Serum (FBS) was purchased from Thermo Scientific HyClone (Waltham, MA, USA). Penicillin-streptomycin solution (PS) and 0.25% Trypsin-EDTA solution were purchased from Gibco (Carlsbad, CA, USA).

2.2. Mammalian cell culture, virus infection and overexpression

H1299 cells were cultured in RPMI 1640 medium supplemented with 5% FBS and 1% PS. Cells were grown in a 37 °C incubator supplied with 5% CO_2. For infection experiments, cells were collected by centrifugation at 600 rpm for 5 min, re-suspended in fresh serum-free medium, and approximately 2.5×10^6 cells were seeded into a 60 mm dish.

A monolayer of cells grown to 100% confluency was washed with serum-free medium twice and inoculated with virus at multiplicity of infection (MOI) of approximately 2, unless specified. Cells were incubated at 37 °C with 5% CO_2 before harvested for analysis at specific time points. For time-course experiments, 0 h samples were harvested after the cells were incubated for 5 min.

Vaccinia/T7 recombinant virus, used for overexpression of genes, was prepared by infecting Vero cells and harvested by three freeze-thaw cycles, as described previously (J. Wang et al., 2009). H1299 cells were grown to 80–90% confluency and infected with the virus for 1 h at 37 °C, 5% CO_2. Plasmid DNA was delivered into the infected cells with Effectene® transfection reagent. The cells were incubated with the transfection mix for 20 h in 37 °C before being lysed.

2.3. Polymerase chain reaction (PCR) and site-directed mutagenesis

Amplification of DNA not exceeding 2000 base pairs (bp) was achieved using KAPA *Taq* DNA polymerase (Kapa Biosystems Inc, USA) or Fermentas *Taq* DNA polymerase (Thermo Scientific, USA). In a 50 µl reaction, 150 ng of template DNA was mixed with 1.5 pmol of each primer, 2 nmol of each dexoyribonucleotide triphosphate, 1 mM $MgSO_4$ and 1.5 U of KOD Hot Start DNA polymerase. Eighteen thermal cycles were used for amplification and each product was purified, digested with *DpnI* to remove template DNA and purified again before transformation for selection.

2.4. In vitro transcription and labeling of RNA probes

All biotin-labeled probes used in biotin pull-down assay were transcribed with PCR products using appropriate primer pairs, as described previously (Tan et al., 2012). A stretch of poly T is included in the 5′ end of reverse primers for the templates of positive sense RNA or forward primers for the templates of negative sense RNA, so that the in vitro transcribed RNA will contain a stretch of poly A tail to facilitate RNA stability. Briefly, a template for EGFP (-) was amplified from pEGFP-N1 using pT-EGFP_F (5′-TTTTTTTTTTTTTTTTTTTTTTGTATGGTGAGCAAGGGCGAGG-3′) and T7-EGFP_510-528R (5′-TGTAATACGACTCACTATAGGGCTGCCGTCCTCGATGTTG-3′). IBV 5′-UTR (+) and IBV 5′-UTR (-) probes were generated from PCR fragments amplified from plasmid pKT-IBVA with the primer pairs T7_i1-27 (5′-TGTAATACGACTCACTATAGGACTTAAGATAGATATTAATATATATCT-3′)/ pT_i507-528R (5′-TTTTTTTTTTTTTTTTTTTTTGTTGTCACTGTCTATTGTATGT-3′) and pT_i1-29 (5′-TTTTTTTTTTTTTTTTTTTTTTACTTAAGATAGATATTAATATATATGTAT-3′)/T7_i528-506R (5′-TGTAATACGACTCACTATAGGGTTGTCACTGTCTATTGTATGTC-3′), respectively. IBV 3′-UTR (+) probe was transcribed from the PCR product amplified from pGEM T easy-IBVE plasmid with primers T7_i27106-27125 (5′-TGTAATACGACTCACTATAGGGTAACATAATGGACCTGTTG-3′) and LDX30 (5′-TGATGCCGGCCACGATGCGTC-3′).

For in vitro transcription, template DNA fragments were purified and eluted in RNase-free water. Linearized plasmid DNA (1 µg) or PCR fragment (200 ng) was incubated with 10 U T7 RNA polymerase, 10 U Protector RNase Inhibitor and NTPs (1 mM each of ATP, CTP, GTP, UTP) in 1X transcription buffer provided with the polymerase, at 37 °C for 2 h. The transcription mix was incubated with 5 U of DNase I at 37 °C for 15 min to remove template DNA. For labeling of RNA products, NTPs were replaced with Biotin RNA Labeling Mix (1 mM each of ATP, CTP, GTP, 0.65 mM UTP, 0.35 mM biotin-16-UTP). Transcripts

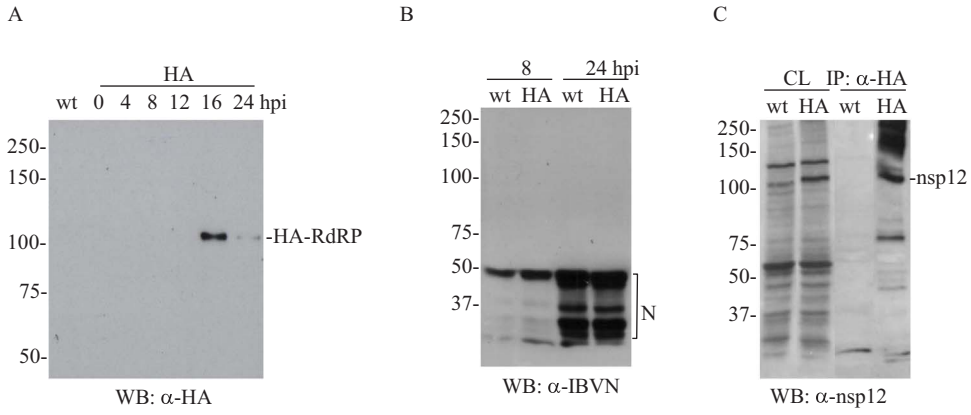

Fig. 1. Construction and characterization of a recombinant IBV expressing HA-tagged RdRP (rIBV-HA-RdRP). a. Kinetic analysis of HA-RdRP expression in cells infected with rIBV-HA-RdRP. Confluent H1299 cells were infected with approximately 2 MOI of wild type IBV (wt) and rIBV-HA-RdRP (HA), respectively. Cells infected with rIBV-HA-RdRP were harvested at 0, 4, 8, 12, 16 and 24 h post-infection, respectively. As a control, cells infected with wild type IBV were harvested at 16 h post-infection. Total cell lysates were prepared, and proteins were separated on 8% SDS-PAGE and analyzed by Western blot with anti-HA antibodies. Numbers on the left indicate protein sizes in kilodalton. b. Replication of rIBV-HA-RdRPin H1299 cells. Confluent H1299 cells were infected with approximately 2 MOI of wild type IBV (wt) and rIBV-HA-RdRP (HA), respectively. The infected cells were harvested at 8 and 24 h post-infection, respectively. Total cell lysates were prepared, proteins were separated on 15% SDS-PAGE and analyzed by Western blot with anti-N antisera. Numbers on the left indicate protein sizes in kilodalton. c. Immunoprecipitation of HA-nsp12 in rIBV-HA-RdRP-infected H1299 cells with HA-beads. Confluent H1299 cells were infected with approximately 2 MOI of wild type IBV (wt) and rIBV-HA-RdRP (HA), respectively. The infected cells were harvested at 16 h post-infection and total cell lysates were prepared. Proteins in the total cell lysates were either separated on 15% SDS-PAGE directly or subjected to immunopecipitation with anti-HA beads before being loaded onto the gel. Analysis of HA-nsp12 expression and immunoprecipitation efficiency was done by Western blot with anti-nsp12 antisera. Numbers on the left indicate protein sizes in kilodalton.

were purified with phenol:chloroform:isoamyl alcohol (25:24:1, v/v) and stored at −80 °C.

2.5. Biotin pull-down assay

All proteins used in this assay were whole cell lysates prepared from Vaccinia/T7-infected H1299 cells over-expressing N-terminal FLAG-epitope tagged proteins. EGFP over-expressed with the same method was used as a negative control. In a 200 µl binding reaction, 0.1 µM of biotin-labeled RNA was mixed with 150 µl of total cell lysate in the presence of 10 mM DTT, 20 µg of yeast tRNA, 200 U of RNase inhibitor and nuclease-free water. The reaction was incubated at room temperature with gentle rotation for 30 min. 40 µl of streptavidin agarose beads (Sigma-Aldrich, USA) was added directly into the tube and the mixture was incubated at room temperature with gentle rotation for 30 min, and then centrifuged at 1000 rpm for 5 min. 500 µl of RNase P (RP) buffer (50 mM KCl, 1 mM $MgCl_2$, 10 mM HEPES, pH 7.5) were used to wash the beads trice and the buffer was removed thoroughly by gently aspiration after the last wash. 25 µl of 2X SDS loading dye with DTT was mixed with the beads and the mixture incubated at 100 °C for 10 min, cooled at room temperature before loaded onto a PAGE gel of an appropriate concentration.

2.6. Protein electrophoresis and Western blot analysis

Polyacrylamide gels were prepared with 30% acrylamide/bis solution (29:1) in 375 mM Tris and 0.1% SDS. The electrophoresis was performed with 1X Tris-Glycine running buffer (25 mM Tris, 250 mM glycine, 0.1% SDS). Resolved proteins were visualized by 30 min of coomassie blue staining (0.25% (w/v) Coomassie Brilliant Blue R-250, 20% methanol, 10% glacial acetic acid) or transferred onto a membrane for immune-detection. Gels were equilibrated in 1X wet transfer buffer (48 mM Tris, 39 mM glycine, 20% methanol) before transferred onto either nitrocellulose or PVDF membranes. Transfer was performed in 1X wet transfer buffer at 4 °C. Membrane was blocked in blocking solution (10% (w/v) non-fat milk in 1X PBS) for 1 h at room temperature and incubated with the primary antibody at an appropriate concentration for 1 h. The membrane was washed with PBS-T (1X PBS, 0.1% Tween®-20) three times and incubated with secondary antibody at a 1:2000 dilution for 1 h. The membrane was washed with PBS-T three times and Western Lightning®-ECL from Perkin Elmer (Waltham, MA, USA) was applied onto the membrane for detection.

2.7. Construction of IBV nsp12 truncation mutants

All nsp12 truncation mutants were created by amplification of the desired fragment from pXL-IBVC, which contained the IBV genome from nucleotide 8689–15526. Fragments amplified with primer pairs i12339-12360_BamHIF (5'-TTGGATCCGAATTATTTAAACGGGTACGGG-3') / i13538_13516_XhoIR (5'-TTCTCGAGTTATAACGCACAAACACTAAAACAAG-3'), i13296-13316_BamHIF (5'-TTGGATCCATACCGCAGACTTCTTTCGGT-3') / i14498-14474_XhoIF (5'-TTCTCGAGTTAGCTCTTAATATTATCATAGACAATA-3') and i13926-13948_BamHIF (5'-TTGGATCCAAGAAGAATGTCCTACCCACTAT-3') / i15128-15106_XhoIR (5'-TTCTCGAGTTATTGTAAAGTCGTAGGAGCTCTAT-3') were cloned into vector pXJ40-Myc generating plasmids that could express N-terminally tagged proteins Myc-iNsp12n, Myc-iNsp12m, Myc-iNsp12c.

3. Result

3.1. Construction and characterization of a recombinant IBV expressing an HA-epitope tagged nsp12

A recombinant IBV which expressed an N-terminally HA-epitope tagged nsp12 (rIBV-HA-RdRP) was constructed using reverse genetics (Fang et al., 2008, 2007, 2010). The HA tag was inserted at nucleotide position 12319 which is two amino acids downstream of the cleavage site between nsp10 and nsp11/12. The recovered recombinant virus grew well in H1299 cells.

Approximately 2 MOI of wild type and the recombinant IBV, respectively, were used to infect confluent H1299 cells. The infected cells were harvested at 24 h post-infection and total cell lysates were prepared. The expression kinetics of the HA-tagged nsp12 in cells infected with rIBV-HA-RdRP was studied in a time-course experiment. H1299 cells infected with the virus were harvested at 0, 4, 8, 12, 16 and 24 h post-infection, respectively, and analyzed by Western blot with anti-HA monoclonal antibodies. Cells infected with wild type IBV harvested at 16 h post-infection were also included as a control. The HA-tagged nsp12 was initially detected at 12 h post-infection and peaked at 16 h post-infection (Fig. 1a). As expected, the same band was not observed in cells infected with wild type IBV (Fig. 1a).

Cells infected with wild type and the recombinant rIBV-HA-RdRP harvested at 8 and 24 h post-infection were also analyzed by Western blot for the expression level of IBV N protein with anti-N antisera. As shown in Fig. 1b, N protein expression was observed in cells infected with both wild type IBV and rIBV-HA-RdRP. In fact, slightly higher level of N protein expression was detected in cells infected with rIBV-HA-RdRP (Fig. 1b), indicating that tagging of RdRP with an HA epitope

does not affect IBV replication in cells.

The expression of wild type and HA-tagged nsp12 in these infected cells as well as the immunoprecipitation efficiency and specificity of HA-tagged nsp12 with α-HA coated beads (HA-beads) were then determined by Western blot with a rabbit polyclonal antiserum against nsp12 (α-RdRP). This was done to ensure that HA-tagged nsp12 could be efficiently pulled-down for detection of other co-precipitated viral and cellular proteins. As can be seen in Fig. 1c, a comparable level of wild type and HA-tagged nsp12 was detected in cells infected with the respective viruses, but only HA-nsp12 was precipitated by HA-beads.

3.2. Screen for non-structural proteins that interact with nsp12

We then decided to identify viral structural, non-structural and accessory proteins that were co-precipitated with the HA-tagged RdRP by Western blot with available antisera. Confluent H1299 cells grown in 80 cm^2 flasks were infected with wild-type and rIBV-HA-RdRP, respectively, and harvested at 16 h post-infection by lysis with 800 μl of Lysis Buffer for each flask. HA-beads (20 μl of 50% slurry) were added to 500 μl of each lysate to precipitate HA-nsp12 and any other interacting proteins from the lysates. The bound proteins were eluted with 55 μl of 2X SDS loading dye and resolved by 8% and 15% SDS-PAGE gel. Because similar numbers of cells were used for infection and virus replication was comparable, the protein levels of host housekeeping genes were similar in cells infected with wild-type rIBV and rIBV-HA-RdRP, as determined by Western blot analysis of GAPDH and β-actin (data not shown). As shown in Fig. 1c, HA-tagged nsp12 could be specifically detected in the cell lysate and co-precipitated samples in cells infected with rIBV-HA-RdRP but not in cells infected with wild-type rIBV. Detection of co-precipitated proteins was performed by Western blot using available antisera for IBV nsps as well as structural proteins S and N. We noted that some antisera (especially α-nsp15) picked up one or more non-specific bands. Only if the target protein of correct molecular weight was detected at similar levels in the whole cell lysates, but could only be detected in the co-immunoprecipitated sample from rIBV-HA-RdRP-infected cells, it would be considered to be a potential interacting partner of HA-tagged nsp12.

The results of the co-immunoprecipitation were presented in Fig. 2. For the structural proteins, S protein was not detected in the immunoprecipitated samples, while a similar level of N was detected in cells infected with wild type IBV and rIBV-HA-RdRP (HA) (Fig. 2, panels anti-IBV S and N). Although it appeared that the amount co-precipitated in rIBV-HA-RdRP-infected samples was slightly higher compared to wild type IBV infected samples, the amount detected in the cell lysates was also slightly higher. So it was unlikely for N to have been specifically co-precipitated by an interaction with nsp12. Nsp3, nsp5, nsp8 and nsp14, but not nsp10, nsp13 and nsp15/nsp16, were specifically detected in the precipitated samples of rIBV-HA-RdRP-infected cells (Fig. 2). As previously reported, a dominant band with an apparent molecular weight of 58 kDa could be detected by Western blot in cells infected with wild type IBV with anti-nsp14 antiserum (Fang et al., 2007). This was proved to be a nonspecific band from our previous work (Xu et al., 2010). As nsp14 band is usually very weak and migrates on SDS-PAGE gel just below this non-specific band, much more samples were added during precipitation and gel loading, leading to the detection of a specific band representing nsp14 in HA-beads precipitated samples (Fig. 2). However, this band cannot be separated from the non-specific band in total cell lysates (Fig. 2). Anti-nsp13 antibodies failed to detect a specific band representing nsp13 either in total cell lysates or in HA-beads precipitated samples (Fig. 2). This issue will be further studied by using a recombinant virus with HA-tagged nsp13 (Zhai et al., 2005).

Additional higher molecular weight bands were also detected in HA-beads precipitated samples with anti-nsp8 and anti-nsp10 antisera, although a specific band representing the nsp10 was not detected (Fig. 2). Based on their apparent molecular masses, these higher molecular weight bands were likely partially processed products of pp1a or pp1ab, which included nsp8 and nsp10, respectively, and thus were detected by the antibodies. Many antisera used during this screening were unable to detect their corresponding protein bands in the cell lysates, due to the low expression level of these proteins during IBV infection in addition to the low levels of antibodies in the sera.

3.3. Further confirmation of the interaction between nsp8 and nsp12

To further confirm that nsp8 interacts with nsp12, immunoprecipitation of nsp12 was repeated with HA-beads. In addition, a reciprocal precipitation was performed using anti-nsp8 serum. The lysates were prepared and the bead-bound proteins were eluted with 2X SDS loading dye and resolved by 8% and 15% SDS-PAGE gels. As shown in Fig. 3A, HA-nsp12 was detected in cells infected with rIBV-HA-RdRP after precipitation with anti-nsp8 serum. Similarly, precipitation of cell lysates with anti-HA antibodies led to the co-precipitation of nsp8 in cells infected with the recombinant virus (Fig. 3B). It was also noted that a dominant band with an apparent molecular weight of 64 kDa was detected in both total cell lysates and in precipitated samples from rIBV-HA-RdRP-infected cells (Fig. 3B). This may represent the cleavage intermediate covering nsp7/8/9/10. Although the interaction between nsp8 and nsp12 has been reported before for SARS-CoV (von Brunn et al., 2007), it was not reported in other coronaviruses and the interaction has not been subjected to an in-depth study. In the subsequent sections, the interaction between these two proteins was further characterized.

3.4. Interaction between nsp8 and nsp12 in the absence of other viral structural and non-structural proteins

The physical interaction between nsp8 and nsp12 was further studied by co-expression of the two proteins in the absence of other viral proteins and viral genomic RNA. The proteins were co-expressed as a FLAG-tagged protein for nsp8 (FLAG-nsp8) and a Myc-tagged protein for nsp12 (Myc-nsp12) in H1299 cells. As controls, dual vector transfected samples (FLAG + Myc) and single vector transfected samples (FLAG-nsp8 + Myc and FLAG + Myc-nsp12) were included. Immunoprecipitation was performed with anti-Myc coated beads (Myc-beads) and the bound proteins were resolved by SDS-PAGE. Western blot was then performed using anti-FLAG-HRP and anti-Myc-HRP antibodies to detect the precipitated proteins. As shown in Fig. 4, FLAG-nsp8 was detected at almost equal amounts whether it was expressed together with Myc only (FLAG-nsp8 + Myc) or with Myc-nsp12 (FLAG-nsp8 + Myc-nsp12), but was detected in the Myc pulled-down samples only when it was co-expressed with Myc-nsp12 (Fig. 4, left panel). The ~ 50 kDa band detected in all immunoprecipitated samples was likely to be the heavy chain eluted from the beads during sample preparation for SDS-PAGE. Also, Myc-nsp12 was detected in both the cell lysates and immunoprecipitated samples (Fig. 4, right panel). As FLAG-nsp8 in the immunoprecipitated sample was detected only when Myc-nsp12 was co-expressed, it was concluded that FLAG-nsp8 was coprecipitated with Myc-nsp12 by interacting with it. These results confirm that nsp12 could interact with nsp8 in the absence of other viral proteins and viral genomic/subgenomic RNAs.

3.5. Effect of RNase A treatment on the interaction between nsp8 and nsp12

We then tested if treatment of cell lysates with RNase A would affect the interaction between the two proteins. For this purpose, immunoprecipitation was performed with cell lysates that were either treated (+RNase A) or not treated (-RNase A) with 50 μg/ml of RNase A at 37 °C for 1 h before adding anti-Myc (Myc-beads) or anti-FLAG (FLAG-beads) coated beads. As shown in Fig. 5A, nsp8 was still precipitated when RNA was removed, suggesting that the interaction between the two proteins is not mediated through their simultaneous

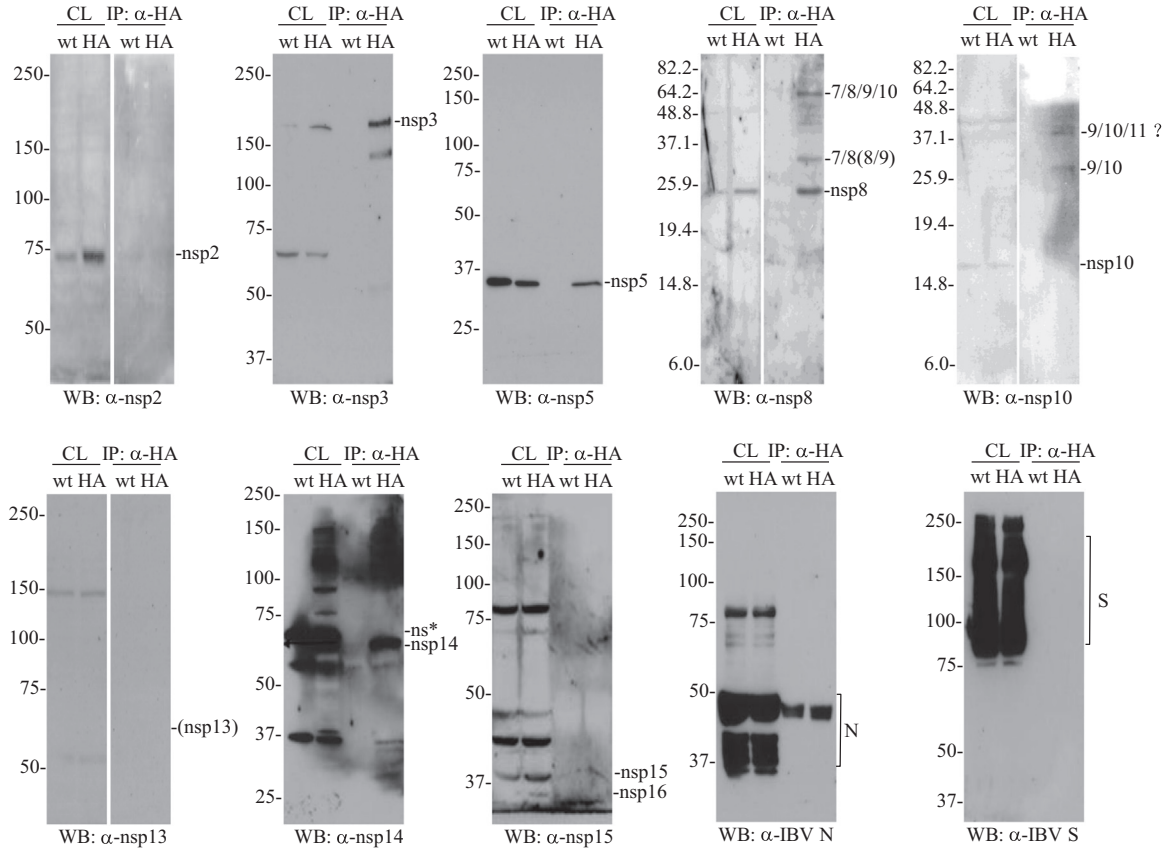

Fig. 2. Co-precipitation IBV non-structural proteins with HA-nsp12 in rIBV-HA-RdRP-infected H1299 cells. Confluent H1299 cells were infected with approximately 2 MOI of wild type IBV (wt) and rIBV-HA-RdRP (HA), respectively. The infected cells were harvested at 16 h post-infection and total cell lysates were prepared. Proteins in the total cell lysates were either separated on 8% and 15% SDS-PAGE directly or subjected to immunopecipitation with anti-HA beads before being loaded onto the gel. IBV proteins expressed in the infected cells and co-precipitated with HA-nsp12 were analyzed by Western blot with antisera specified under each panel. Antisera which were used but not presented were for the following proteins: nsp7, ORF 3a, ORF 3b, ORF 5a and E. A representative result of two independent experiments was shown. Numbers on the left indicate protein sizes in kilodalton, and the identities of the IBV proteins are indicated on the right.

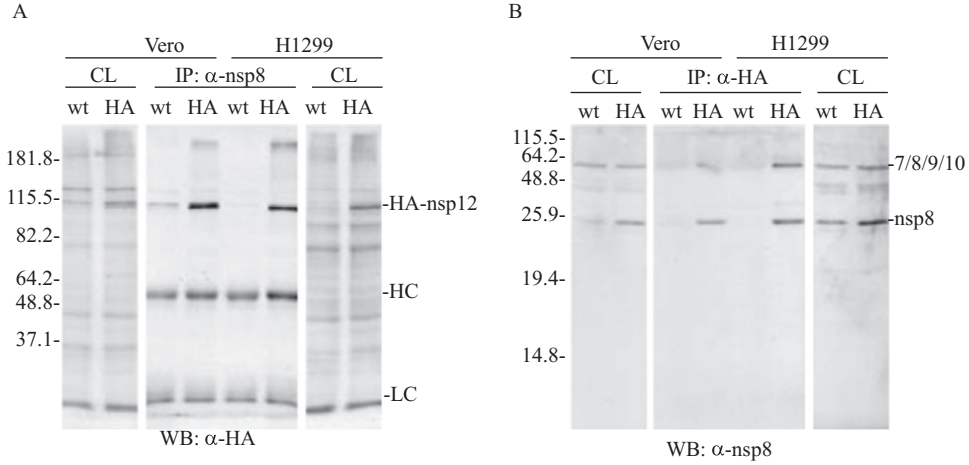

Fig. 3. Coprecipitation of IBV nsp8 with HA-nsp12 and vice versa in both Vero and H1299 cells. a. Confluent H1299 and Vero cells were infected with approximately 2 MOI of wild type IBV (wt) and rIBV-HA-RdRP (HA), respectively. The infected cells were harvested at 16 h post-infection and total cell lysates were prepared. Proteins in the total cell lysates were either separated on 8% SDS-PAGE directly or subjected to immunopecipitation with anti-nsp8 antiserum before being loaded onto the gel. Analysis of the expression of HA-nsp12 and the immunoprecipitation efficiency was done by Western blot with anti-HA antibodies. Numbers on the left indicate protein sizes in kilodalton. b. Confluent H1299 and Vero cells were infected with approximately 2 MOI of wild type IBV (wt) and rIBV-HA-RdRP (HA), respectively. The infected cells were harvested at 16 h post-infection and total cell lysates were prepared. Proteins in the total cell lysates were either separated on 15% SDS-PAGE directly or subjected to immunopecipitation with anti-HA beads before being loaded onto the gel. Analysis of the expression of nsp8 and the immunoprecipitation efficiency was done by Western blot with anti-nsp8 antibodies. Numbers on the left indicate protein sizes in kilodalton.

interactions with RNA. Similar result was also obtained in the reciprocal co-immunoprecipitation using anti-FLAG antibody (Fig. 5B). A low level of Myc-nsp12 was detected in the whole cell lysate, due to the loading of the small amount of cell lysate as input, as compared with the large amount of cell lysate used for co-immunoprecipitation. The two reciprocal co-immunoprecipitation experiments thus confirmed that nsp8 interacts directly with nsp12 and further supported that this interaction is not dependent on the presence of the genomic and subgenomic viral RNA.

3.6. Nsp8 interacts with the N- and C-terminal regions of nsp12

We then set up to map the domain(s) on nsp12 responsible for the interaction between the two proteins. Three Myc-tagged deletion mutants of nsp12 were created, as shown in Fig. 6a. Because the truncated mutants encode peptide fragments with up to 400 amino acid residues,

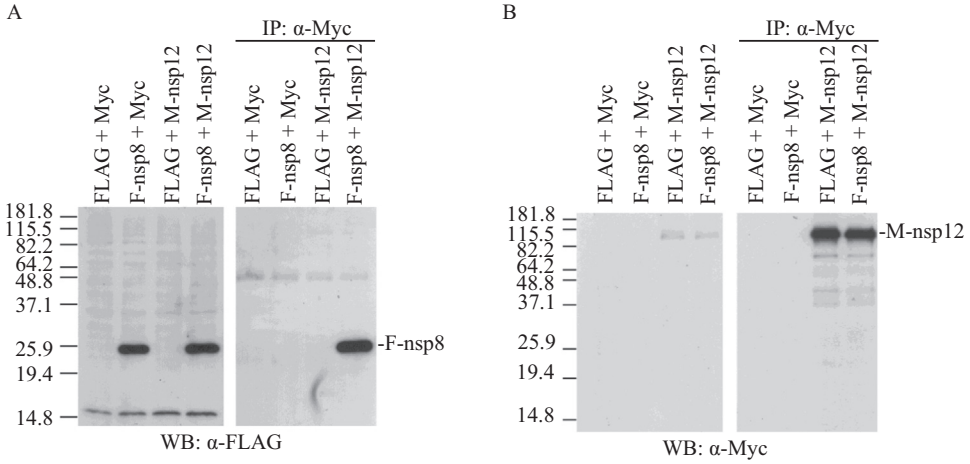

Fig. 4. Formation of FLAG-nsp8 and Myc-nsp12 complex in cells over-expressing the two epitope-tagged proteins. H1299 cells were grown to 80% confluency and infected with Vaccinia/T7 recombinant virus for 1 h at 37 °C, 5% CO_2. Plasmid DNA was delivered into the infected cells with Effectene® Transfection Reagent. The cells were incubated with the transfection mix for 20 h in the 37 °C incubator before they were lysed with Lysis buffer. Total cell lysates were either separated on 15% SDS-PAGE directly or subjected to immunopecipitation with anti-Myc beads before being loaded onto the gel. Analysis of the expression of the over-expressed proteins and their co-immunoprecipitation was done by Western blot with anti-FLAG (A) and anti-Myc (B) antibodies, respectively. Numbers on the left indicate protein sizes in kilodalton.

we hypothesized that critical domains and/or protein folding motifs would remain intact, and thus the structural features and stability of the mutants would not be drastically affected. The three mutants encode IBV nsp12 fragments with considerable overlaps, to ensure that potential nsp8 interacting domain(s) disrupted by the margin of a fragment would still remain intact in another mutant.

The three mutants and full-length nsp12 (Myc-nsp12) were either co-expressed with FLAG-nsp8. The cell lysates were probed to assess the expression levels of the different nsp12 mutants. As shown in Fig. 6b (left), full-length Myc-nsp12 was detected at high levels in transfected cells. Protein levels of Myc-nsp12n and Myc-nsp12c were slightly lower, while that of Myc-nsp12m was considerably lower compared with the full-length protein, suggesting that the deletion mutants were not as stable as the full-length protein. The cell lysates were also precipitated with FLAG-beads and the bound proteins were resolved by SDS-PAGE and detection was made with anti-Myc-HRP antibody. As expected, the full-length Myc-nsp12 interacted strongly with FLAG-nsp8 and was efficiently co-precipitated. On the other hand, the level of co-precipitated protein was lower for Myc-nsp12n and considerably lower for Myc-nsp12c, compared with that of full-length nsp12. No detectable level of Myc-nsp12m could be co-precipitated (Fig. 6b, right). Therefore, the nsp8 interacting domain(s) in nsp12 was attributed mainly by the N-terminal region, and to a lesser degree by the C-terminal region, but not its middle region. The absence of Myc-tagged protein co-precipitation in samples which were co-expressed with FLAG-epitope, indicated that the co-precipitation of Myc-nsp12n and Myc-nsp12c were dependent on the presence and their interaction with FLAG-nsp8, as was the case for Myc-nsp12.

3.7. Biotin pull-down screen for RNA-binding activity of IBV non-structural proteins

Plasmids based on the vector pXJ40-FLAG inserted with nucleotide sequences of nsps either in tandem (nsp7/8 fusion and nsp8/9 fusion) or individually were used to over-express the proteins in Vaccinia/T7 virus-infected H1299 cells. Due to either the very low expression efficiency or the lack of distinctive band, the screen data for nsp3, nsp4, nsp6 and nsp13 were not included. Total cell lysates were used in biotin pull-down assays with biotinylated 5′-UTR (+), 5′-UTR (-) or 3′-UTR (+) RNA probes. As the focus of the study was on negative strand RNA synthesis, only the positive sense UTRs and the 5′-UTR (-), which contains the anti-leader TRS important for strand-transfer during discontinuous transcription of negative strands, were included in the screen. The proteins bound to the streptavidin beads were resolved by SDS-PAGE and detected by Western blot using anti-FLAG-HRP antibody. EGFP was also included as a non-binding protein negative control

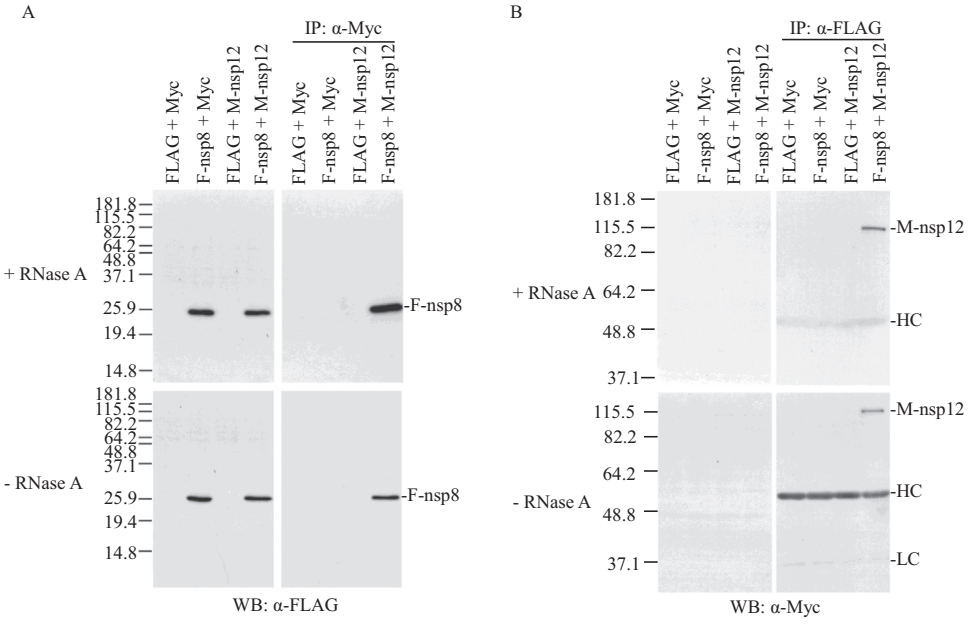

Fig. 5. Co-precipitation of FLAG-nsp8 and Myc-nsp12 in total cell lysates with or without RNase A treatment. H1299 cells were grown to 80% confluency and infected with Vaccinia/T7 recombinant virus for 1 h at 37 °C, 5% CO_2. Plasmid DNA was delivered into the infected cells with Effectene® Transfection Reagent. The cells were incubated with the transfection mix for 20 h in the 37 °C incubator before they were lysed with Lysis buffer. A portion of the lysates was treated with 50 μg/ml of RNase A at 37 °C for 1 h. Both treated and untreated cell lysates were either separated on 8% and 15% SDS-PAGE directly or subjected to immunopecipitation with anti-Myc (A) and anti-FLAG (B) beads, respectively before being loaded onto the gel. Analysis of the expression of the over-expressed proteins and their co-immunoprecipitation was done by Western blot with anti-FLAG (A) and anti-Myc (B) antibodies, respectively. Numbers on the left indicate protein sizes in kilodalton.

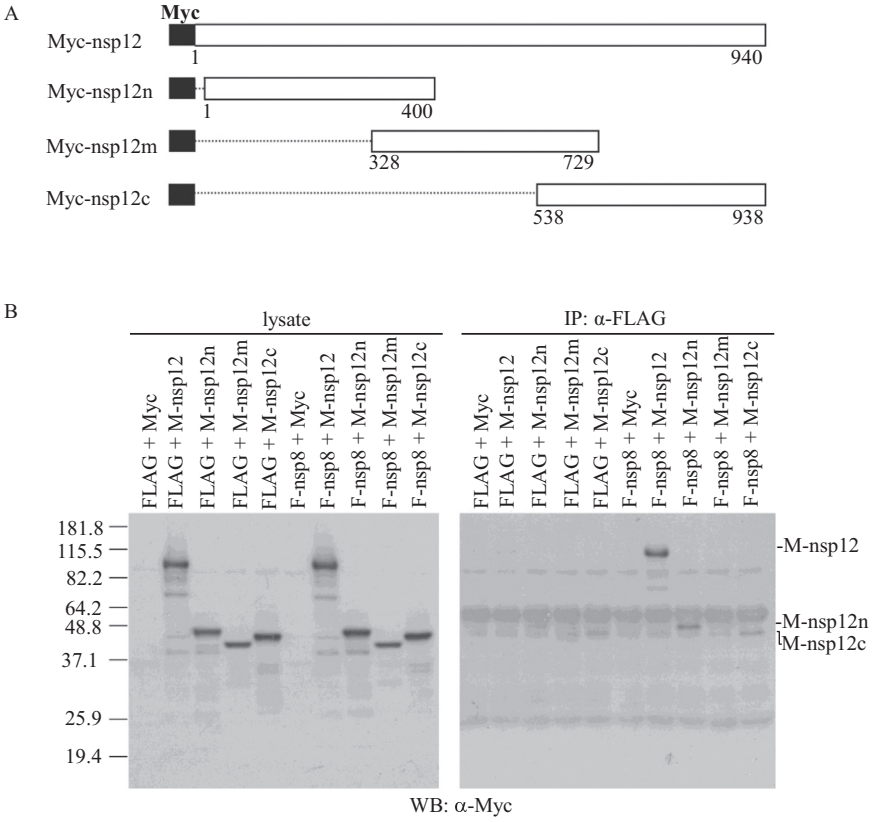

Fig. 6. Mapping the regions on nsp12 responsible for interaction with nsp8. a. Schematic diagram of Myc-tagged nsp12 truncation mutant proteins. Numerals indicate amino acid positions. b. The N- and C-terminal portions of IBV nsp12 co-precipitated with FLAG-nsp8 using FLAG-beads. Full-length and truncated nsp12 proteins or Myc (vector control) were co-expressed with FLAG (vector control) or FLAG-nsp8. The cell lysates were precipitated with FLAG-beads and bound proteins were analyzed with western blotting using α-Myc. Full-length nsp12 and mutants nsp12n (residues 9 – 400), nsp12c (residues 538 – 938) were co-precipitated by the beads. A representative result of three independent experiments was shown.

in each screen. For the screen conducted using biotinylated IBV 5′-UTR (+), individual nsps, two fusion proteins, nsp7/8 and nsp8/9, and EGFP were over-expressed in H1299 cells infected with Vaccinia/T7 recombinant virus on 60 mm dishes. Cells were lysed with 250 μl of Lysis Buffer and used immediately. Biotin pull-down assay was performed with 0.1 μM (final concentration) biotinylated IBV 5′-UTR (+) probe with 150 μl cell lysate, and streptavidin beads were used to purify the biotinylated RNA from the mixture. Proteins bound to the beads through interactions with the bound RNA were eluted with 2X SDS loading dye. For Western blot analysis, 10 μl of cell lysate and all of the eluted proteins were denatured and resolved by SDS-PAGE. Detection of the FLAG-tagged nsps and EGFP were performed with anti-FLAG-HRP and anti-EGFP antibodies, respectively. As shown in Fig. 7a, proteins that were able to co-purify with the biotinylated probe in the assay were nsp2, nsp10 and to a lesser extent, nsp5.

Similar biotin pull-down assays with biotinylated 5′-UTR (-) and 3′-UTR (+) probes were performed to screen for interacting proteins. Proteins which co-purified with the biotinylated 5′-UTR (-) RNA probe were nsp2, nsp5 and nsp10 (Fig. 7b). Nsp2, nsp5, nsp8 and nsp9 were shown to be interacting with the biotinylated 3′-UTR (+) probe (Fig. 7c). Among them, nsp5 showed strong interaction, nsp2, nsp8 and nsp9 showed a moderate level of interaction with IBV 3′-UTR (Fig. 7c).

4. Discussion

In this study, we have shown that IBV nsp12 is able to complex with a number of other non-structural proteins, including nsp3, nsp5, nsp8 and nsp14. Further characterization of the nsp8-nsp12 complex demonstrated that the formation of this complex is independent of the 5′- and 3′-UTRs of viral RNA and other nsps. Nsp8 interacts with nsp12 at two points, both the N- and C-terminial regions of the protein. Analysis of viral RNA-protein interactions using the biotin pull-down assay revealed that nsp2, nsp8, nsp9 and nsp10 exhibit RNA-binding activity to either of the UTRs. The efforts to draw a more complete picture were hampered by the difficulty of expressing/detecting certain nsps, such as nsp4 and nsp13, as well as the insolubility of nsp6, a protein containing multiple transmembrane domains (Oostra et al., 2008).

One previously undocumented interaction between nsp2 and viral RNA was founded by the screen. This finding adhered to a previous report of nsp2 possibly being a weak antagonist of PKR (X. Wang et al., 2009), which requires double-stranded RNA for activation. The screen also showed that nsp9 and nsp10 only bind to some but not all three probes tested. This is unexpected as both proteins were previously documented to have RNA-binding activities with a non-specific nature (B. Chen et al., 2009; Egloff et al., 2004; Joseph et al., 2006). This could, however, be explained by the generally weak interactions of these two proteins and the RNA probes that could escape detection in one or more of the screens. The interaction between nsp8 and IBV 3′-UTR (+) may have provided another piece of evidence that nsp8 is heavily involved in viral RNA synthesis, as a RNA-primer synthesizing enzyme for nsp12. It should also be noted that the observed differential interactions of these nsps with UTRs in cells overexpressing these proteins may be due to the fact that the amounts of the over-expressed nsps may be likely rather different from those expressed in virus-infected cells.

Attempts to depict a more complete map of viral protein-protein interactions were also hampered by the limited availability of sensitive antisera to some viral proteins, especially those of the less immunogenic nsps and accessory proteins. Compounded by the fact that many non-structural and accessory proteins were expressed in much lower amounts compared to structural proteins, their detection in cell lysates proved to be much more difficult. Out of the six nsps which could be detected by the available antisera, nsp3, nsp5, nsp8 and nsp14 were identified as binding partners to nsp12. Nsp8-nsp12 interaction was reported in an ORFeome screen for SARS-CoV (von Brunn et al., 2007). Since it has not been proven to exist in other coronaviruses, reporting the same interaction in IBV suggests that it is highly probable that the interaction holds true for all other coronaviruses.

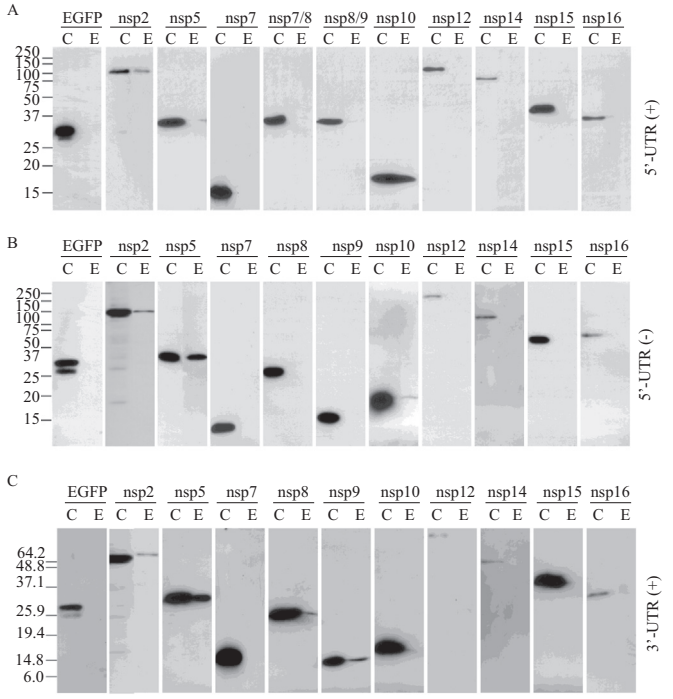

Fig. 7. Screen for IBV non-structural proteins that interact with the 5′-UTR (+), 5′-UTR (-) and 3′-UTR (+) of IBV. a. IBV nsp2, nsp5 and nsp10 showed binding activity to its 5′-UTR (+). Biotin pull-down assay of non-structural proteins with IBV 5′-UTR (+). Cell lysates of H1299 cells over-expressing different non-structural proteins were incubated with biotinylated 5′-UTR (+) probes and purified using streptavidin beads. Bound proteins were resolved by SDS-PAGE and western blot was performed. Proteins which did not express were not presented. C: cell lysate, E: elution. A representative result of two independent experiments was shown. b. IBV nsp5 and nsp10 showed binding activity to its 5′-UTR (-). Biotin pull-down assay of non-structural proteins with IBV 5′-UTR (-). Cell lysates of H1299 cells over-expressing different non-structural proteins were incubated with biotinylated 5′-UTR (-) probes and purified using streptavidin beads. Bound proteins were resolved by SDS-PAGE and western blot was performed. The expression of nsp2 was not detectable for this assay and was excluded. C: cell lysate, E: elution. A representative result of two independent experiments was shown. c. IBV nsp5, nsp8 and nsp9 showed binding activity to IBV 3′-UTR (+). Biotin pull-down assay of non-structural proteins with IBV 3′-UTR (+). Cell lysates of H1299 cells over-expressing different non-structural proteins were incubated with biotinylated 3′-UTR (+) probes and purified using streptavidin beads. Bound proteins were resolved by SDS-PAGE and western blot was performed. C: cell lysate, E: elution. A representative result of two independent experiments was shown.

The nsp8 binding activity in nsp12 appeared to be present in both Myc-nsp12n and Myc-nsp12c, its N- and C-terminally truncated mutants. Coincidentally, it was reported for SARS-CoV that both a p12 fragment in its N-terminal and a p64 fragment in its C-terminal regions were required for the RdRP activity of nsp12 (Cheng et al., 2005). The p12 and p64 fragments were shown to form a stable complex and the p12 fragment may play a role in primer-binding while the p64 fragment contains the polymerase activity. Therefore, the ability of nsp8 to interact with Myc-nsp12n (residues 9–400) seemed to add a piece of supporting evidence for the role of the p12 fragment in primer-binding. This offers an interesting perspective on the coordination between coronavirus nsp8 and nsp12 in viral RNA synthesis.

Information pertaining to how the initiation of coronavirus negative-strand synthesis is limited and only in the recent years has more information been available with regards to the source of the primer required for RdRP (nsp12) to be functioning (te Velthuis et al., 2010). The structure of SARS-CoV nsp7-nsp8 complex has been solved by two groups (Zhai et al., 2005; Xiao et al., 2012), revealing a hexadecameric 8:8 complex between the two proteins, and a 2:1 heterotrimer of the two proteins in the crystal as well as in solution, respectively. de novo RNA synthesis has also been demonstrated for nsp7 and nsp8 from both SARS-CoV and feline coronavirus (FeCoV) (Xiao et al., 2012; Velthuis et al., 2012). The nsp7-nsp8 hexadecameric complex which was shown to be the second RdRP of coronavirus requiring no primer to function and synthesizing short length RNA non-specifically fulfilled the role as the primase for nsp12 (Imbert et al., 2006).

A likely, although premature, model that would fit the mapped interactions would indicate a direct interaction between the N- and C-terminal regions of nsp12 with the nsp7-nsp8 complex. In this model, the nsp7-nsp8 complex would first synthesize a RNA-primer of a sufficient length, which would be exposed to and binds to the N-terminal region of nsp12, brought in close proximity through its interaction with nsp8. The extension of the RNA chain could then be catalyzed by the polymerase domain in the C-terminal region of nsp12, which would also be oriented in close proximity to the end of the RNA-primer through its interactions at its N-terminal region with nsp8. This arrangement of the two RdRPs would ensure the high efficiency of the replicase complex as the RNA primers synthesized by nsp8 could be utilized by nsp12 immediately for transcription elongation. This putative model is supported by structural studies showing that nsp8 is a very elongated molecule (Xiao et al., 2012), it could be easily spanning the N- and the C-terminal regions of nsp12. Further characterization of the interaction between nsp8 and nsp12 is required to ascertain if the proposed model is valid. In addition, identification and characterization of the interactions between nsp12 and other nsps as well as the interactions among other nsps would be required to depict a more complete picture of the viral replication/transcription complex. Attempts to co-express all nsps in the same cells were made, but no presentable data were generated, possibly due to the low expression efficiency of several nsps and the even lower expression efficiency when co-expressing them.

Structural information, especially the resolution of the nsp12 structure would be of particular importance in confirming if the interactions detected between its N- and C-terminal regions and nsp8 are spatially possible. However, as the structures of coronavirus nsp12 are not solved till date, only predictions of its structure are available. This would be one of the most important studies required for elucidation of the cooperation between nsp8 and nsp12. Likewise, the interaction site on nsp8 should also be mapped as its interaction with nsp12 would only be meaningful if it is confined to the exterior of the hexadecameric complex. Subissi et al. have identified P183 and R190 on the SARS-CoV nsp8 to be essential for its interaction with SARS-CoV nsp12 (Subissi et al., 2014). It would be interesting to examine whether the corresponding residues in IBV nsp8 is also required for nsp12-binding. In addition, functional studies by introducing mutations at the interaction sites could be performed to ascertain if the interaction between nsp8 and nsp12 is crucial for the processivity of the replicase complex.

Coronavirus nsp9 was shown to be a weak, non-specific single-stranded nucleic acid binding protein (ssDNA and ssRNA) (B. Chen et al., 2009; Egloff et al., 2004). It was interesting that nsp9 was found to interact weakly only with IBV 3′-UTR (+) and not at all with the 5′-UTR in both polarity. There is still a possibility of nsp9 being able to bind particular regions of the coronavirus genome in a sequence specific manner, and 3′-UTR (+) could have been its specific interaction partner. Conversely, the low affinity binding could imply that the weak affinity binding to the biotinylated probe was of a non-specific nature. Further studies would be required to verify the specificity of the interaction.

The actual structure of nsp10 is controversial. In one study, nsp10 is described as a dodecamer, but the same structure was not observed in another study (Su et al., 2006). In fact, no dodecamer formation has been described for this protein in solution (Joseph et al., 2006). Nsp10 is a cofactor for both the 2′O-methyltransferase activity of nsp16, and the N7-guanine-methyltransferase / exoribonuclease activities of nsp14 (Decroly et al., 2008; Bouvet et al., 2012). As a stimulatory factor, nsp10 may enhance the 2′-O-methyltransferase activity of nsp16 which catalyzes the conversion of the cap-0 structure on m7GpppA-RNA to a cap-1 structure (Decroly et al., 2008). Nsp10 was also shown to exhibit low-affinity binding to ssRNA, dsRNA and dsDNA in the absence of

other viral proteins (Joseph et al., 2006). Hence, in a case similar to nsp9, the binding of nsp10 to IBV 5′-UTR (-) could also be of low-specificity.

Nsp2 was found to interact with IBV 5′-UTR (+) and it could not be concluded if it bound to IBV 5′-UTR (-) and 3′-UTR (+). Although nsp2 was not reported to be a RNA-binding protein, it had been demonstrated as a weak antagonist of PKR antagonist (X. Wang et al., 2009), a dsRNA-activated kinase. Although the mechanism of this antagonism has yet to be determined, it is logical to propose that nsp2 might act as a competitive dsRNA-binding protein, preventing PKR from being activated by dsRNA synthesized by the virus during replication and transcription.

It was intriguing to find nsp5 interacting with all three probes tested, of which its interactions with the 5′-UTR (-) and 3′-UTR (+) were rather strong. Nsp5 is a 3C-like protease, one of the proteases involved in the proteolytic processing of the replicase gene products. Having no prior reports of it possessing RNA-binding activity, this represents a novel piece of information with regards to the function of nsp5 in addition to its role as a main protease and would warrant further studies.

Acknowledgement

This work was partially supported by an Academic Research Fund (AcRF) Tier 2 grant (ACR47/14), Ministry of Education, Singapore.

References

Angelini, M.M., Akhlaghpour, M., Neuman, B.W., Buchmeier, M.J., 2013. Severe acute respiratory syndrome coronavirus non-structural proteins 3, 4, and 6 induce double-membrane vesicles. MBio 4 (4), e00524–13.

Bhardwaj, K., Guarino, L., Kao, C.C., 2004. The severe acute respiratory syndrome coronavirus Nsp15 protein is an endoribonuclease that prefers manganese as a cofactor. J. Virol. 78 (22), 12218–12224.

Bouvet, M., Debarnot, C., Imbert, I., Selisko, B., Snijder, E.J., Canard, B., et al., 2010. In vitro reconstitution of SARS-coronavirus mRNA cap methylation. PLoS Pathog. 6 (4), e1000863.

Bouvet, M., Imbert, I., Subissi, L., Gluais, L., Canard, B., Decroly, E., 2012. RNA 3′-end mismatch excision by the severe acute respiratory syndrome coronavirus non-structural protein nsp10/nsp14 exoribonuclease complex. Proc. Natl. Acad. Sci. USA 109 (24), 9372–9377.

Brockway, S.M., Clay, C.T., Lu, X.T., Denison, M.R., 2003. Characterization of the expression, intracellular localization, and replication complex association of the putative mouse hepatitis virus RNA-dependent RNA polymerase. J. Virol. 77 (19), 10515–10527.

von Brunn, A., Teepe, C., Simpson, J.C., Pepperkok, R., Friedel, C.C., Zimmer, R., et al., 2007. Analysis of intraviral protein-protein interactions of the SARS coronavirus ORFeome. PloS One 2 (5), e459.

Chen, B., Fang, S., Tam, J.P., Liu, D.X., 2009. Formation of stable homodimer via the C-terminal alpha-helical domain of coronavirus non-structural protein 9 is critical for its function in viral replication. Virology 383 (2), 328–337.

Chen, Y., Cai, H., Pan, J., Xiang, N., Tien, P., Ahola, T., et al., 2009. Functional screen reveals SARS coronavirus non-structural protein nsp14 as a novel cap N7 methyltransferase. Proc. Natl. Acad. Sci. USA 106 (9), 3484–3489.

Chen, Y., Su, C., Ke, M., Jin, X., Xu, L., Zhang, Z., et al., 2011. Biochemical and structural insights into the mechanisms of SARS coronavirus RNA ribose 2′-O-methylation by nsp16/nsp10 protein complex. PLoS Pathog. 7 (10), e1002294.

Cheng, A., Zhang, W., Xie, Y., Jiang, W., Arnold, E., Sarafianos, S.G., et al., 2005. Expression, purification, and characterization of SARS coronavirus RNA polymerase. Virology 335 (2), 165–176.

Decroly, E., Imbert, I., Coutard, B., Bouvet, M., Selisko, B., Alvarez, K., et al., 2008. Coronavirus non-structural protein 16 is a cap-0 binding enzyme possessing (nucleoside-2′O)-methyltransferase activity. J. Virol. 82 (16), 8071–8084.

Egloff, M.-P., Ferron, F., Campanacci, V., Longhi, S., Rancurel, C., Dutartre, H., et al., 2004. The severe acute respiratory syndrome-coronavirus replicative protein nsp9 is a single-stranded RNA-binding subunit unique in the RNA virus world. Proc. Natl. Acad. Sci. USA 101 (11), 3792–3796.

Fang, S., Chen, B., Tay, F.P.L., Ng, B.S., Liu, D.X., 2007. An arginine-to-proline mutation in a domain with undefined functions within the helicase protein (Nsp13) is lethal to the coronavirus infectious bronchitis virus in cultured cells. Virology 358 (1), 136–147.

Fang, S., Shen, H., Wang, J., Tay, F.P.L., Liu, D.X., 2010 Jul. Functional and genetic studies of the substrate specificity of coronavirus infectious bronchitis virus 3C-like proteinase. J. Virol. 84 (14), 7325–7336.

Fang, S.G., Shen, S., Tay, F.P.L., Liu, D.X., 2005. Selection of and recombination between minor variants lead to the adaptation of an avian coronavirus to primate cells. Biochem. Biophys. Res. Commun. 336 (2), 417–423.

Fang, S.G., Shen, H., Wang, J., Tay, F.P.L., Liu, D.X., 2008. Proteolytic processing of polyproteins 1a and 1ab between non-structural proteins 10 and 11/12 of Coronavirus infectious bronchitis virus is dispensable for viral replication in cultured cells. Virology 379 (2), 175–180.

Imbert, I., Guillemot, J., Bourhis, J., Bussetta, C., Coutard, B., Egloff, M., et al., 2006. A second, non-canonical RNA-dependent RNA polymerase in SARS Coronavirus. EMBO J. 25 (20), 4933–4942.

Imbert, I., Snijder, E.J., Dimitrova, M., Guillemot, J.-C., Lécine, P., Canard, B., 2008 May. The SARS-Coronavirus PLnc domain of nsp3 as a replication/transcription scaffolding protein. Virus Res. 133 (2), 136–148.

Ivanov, K.A., Thiel, V., Dobbe, J.C., van der Meer, Y., Snijder, E.J., Ziebuhr, J., 2004a. Multiple enzymatic activities associated with severe acute respiratory syndrome coronavirus helicase. J. Virol. 78 (11), 5619–5632.

Ivanov, K.A., Hertzig, T., Rozanov, M., Bayer, S., Thiel, V., Gorbalenya, A.E., et al., 2004b. Major genetic marker of nidoviruses encodes a replicative endoribonuclease. Proc. Natl. Acad. Sci. USA 101 (34), 12694–12699.

Joseph, J.S., Saikatendu, K.S., Subramanian, V., Neuman, B.W., Brooun, A., Griffith, M., et al., 2006. Crystal structure of non-structural protein 10 from the severe acute respiratory syndrome coronavirus reveals a novel fold with two zinc-binding motifs. J. Virol. 80 (16), 7894–7901.

Knoops, K., Kikkert, M., Van Den Worm, S.H.E., Zevenhoven-Dobbe, J.C., Van Der Meer, Y., Koster, A.J., et al., 2008. SARS-coronavirus replication is supported by a reticulovesicular network of modified endoplasmic reticulum. PLoS Biol. 6 (9), e226.

Lim, K.P., Liu, D.X., 1998. Characterization of the two overlapping papain-like proteinase domains encoded in gene 1 of the coronavirus infectious bronchitis virus and determination of the C-terminal cleavage site of an 87-kDa protein. Virology 245 (2), 303–312.

Lim, K.P., Ng, L.F., Liu, D.X., 2000. Identification of a novel cleavage activity of the first papain-like proteinase domain encoded by open reading frame 1a of the coronavirus Avian infectious bronchitis virus and characterization of the cleavage products. J. Virol. 74 (4), 1674–1685.

Liu, D., Inglis, S., 1992a. Identification of two new polypeptides encoded by mRNA5 of the coronavirus infectious bronchitis virus. Virology. 186 (1), 342–347.

Liu, D., Inglis, S., 1992b. Internal entry of ribosomes on a tricistronic mRNA encoded by infectious bronchitis virus. J Virol. 66 (10), 6143–6154.

Liu, D., Cavanagh, D., Green, P., Inglis, S., 1991. A polycistronic mRNA specified by the coronavirus infectious bronchitis virus. Virology. 184 (2), 531–544.

Liu, D.X., Brown, T.D., 1995. Characterisation and mutational analysis of an ORF 1a-encoding proteinase domain responsible for proteolytic processing of the infectious bronchitis virus 1a/1b polyprotein. Virology 209 (2), 420–427.

Liu, D.X., Brierley, I., Tibbles, K.W., Brown, T.D., 1994. A 100-kilodalton polypeptide encoded by open reading frame (ORF) 1b of the coronavirus infectious bronchitis virus is processed by ORF 1a products. J Virol. 68 (9), 5772–5780.

Liu, D.X., Tibbles, K.W., Cavanagh, D., Brown, T.D., Brierley, I., 1995. Identification, expression, and processing of an 87-kDa polypeptide encoded by ORF 1a of the coronavirus infectious bronchitis virus. Virology. 208 (1), 48–57.

Liu, D.X., Xu, H.Y., Brown, T.D., 1997. Proteolytic processing of the coronavirus infectious bronchitis virus 1a polyprotein: identification of a 10-kilodalton polypeptide and determination of its cleavage sites. J. Virol. 71 (3), 1814–1820.

Liu, D.X., Shen, S., Xu, H.Y., Wang, S.F., 1998. Proteolytic mapping of the coronavirus infectious bronchitis virus 1b polyprotein: evidence for the presence of four cleavage sites of the 3C-like proteinase and identification of two novel cleavage products. Virology 246 (2), 288–297.

Ma, Y., Wu, L., Shaw, N., Gao, Y., Wang, J., Sun, Y., et al., 2015. Structural basis and functional analysis of the SARS coronavirus nsp14-nsp10 complex. Proc. Natl. Acad. Sci. USA 112 (30), 9436–9441.

Maier, H.J., Hawes, P.C., Cottam, E.M., Mantell, J., Verkade, P., Monaghan, P., et al., 2013. Infectious bronchitis virus generates spherules from zippered endoplasmic reticulum membranes. MBio 4 (5), e00801–e00813.

Minskaia, E., Hertzig, T., Gorbalenya, A.E., Campanacci, V., Cambillau, C., Canard, B., et al., 2006. Discovery of an RNA virus 3′- > 5′ exoribonuclease that is critically involved in coronavirus RNA synthesis. Proc. Natl. Acad. Sci. USA 103 (13), 5108–5113.

Ng, L.F., Liu, D.X., 1998. Identification of a 24-kDa polypeptide processed from the coronavirus infectious bronchitis virus 1a polyprotein by the 3C-like proteinase and determination of its cleavage sites. Virology 243 (2), 388–395.

Ng, L.F., Liu, D.X., 2000. Further characterization of the coronavirus infectious bronchitis virus 3C-like proteinase and determination of a new cleavage site. Virology 272 (1), 27–39.

Ng, L.F.P., Liu, D.X., 2002. Membrane association and dimerization of a cysteine-rich, 16-kilodalton polypeptide released from the C-terminal region of the coronavirus infectious bronchitis virus 1a polyprotein. J. Virol. 76 (12), 6257–6267.

Oostra, M., Hagemeijer, M.C., van Gent, M., Bekker, C.P., te Lintelo, E.G., Rottier, P.J., et al., 2008. Topology and membrane anchoring of the coronavirus replication complex: not all hydrophobic domains of nsp3 and nsp6 are membrane spanning. J. Virol. 82 (24), 12392–12405.

Pan, J., Peng, X., Gao, Y., Li, Z., Lu, X., Chen, Y., et al., 2008. Genome-wide analysis of protein-protein interactions and involvement of viral proteins in SARS-CoV replication. PloS One 3 (10), e3299.

Pasternak, A.O., Spaan, W.J.M., Snijder, E.J., 2006. Nidovirus transcription: how to make sense. . . ? J. Gen. Virol. 87 (Pt 6), 1403–1421.

Ricagno, S., Egloff, M.-P., Ulferts, R., Coutard, B., Nurizzo, D., Campanacci, V., et al., 2006. Crystal structure and mechanistic determinants of SARS coronavirus non-structural protein 15 define an endoribonuclease family. Proc. Natl. Acad. Sci. USA 103 (32), 11892–11897.

Seybert, A., Hegyi, A., Siddell, S.G., Ziebuhr, J., 2000. The human coronavirus 229E

superfamily 1 helicase has RNA and DNA duplex-unwinding activities with 5′-to-3′ polarity. RNA N Y 6 (7), 1056–1068.
Su, D., Lou, Z., Sun, F., Zhai, Y., Yang, H., Zhang, R., et al., 2006. Dodecamer structure of severe acute respiratory syndrome coronavirus non-structural protein nsp10. J Virol. 80 (16), 7902–7908.
Subissi, L., Posthuma, C.C., Collet, A., Zevenhoven-Dobbe, J.C., Gorbalenya, A.E., Decroly, E., et al., 2014. One severe acute respiratory syndrome coronavirus protein complex integrates processive RNA polymerase and exonuclease activities. Proc. Natl. Acad. Sci. USA. 111 (37), E3900–E3909.
Tan, Y.W., Hong, W., Liu, D.X., 2012 Jun. Binding of the 5′-untranslated region of coronavirus RNA to zinc finger CCHC-type and RNA-binding motif 1 enhances viral replication and transcription. Nucleic Acids Res. 40 (11), 5065–5077.
te Velthuis, A.J.W., Arnold, J.J., Cameron, C.E., van den Worm, S.H.E., Snijder, E.J., 2010. The RNA polymerase activity of SARS-coronavirus nsp12 is primer dependent. Nucleic Acids Res. 38 (1), 203–214.
te Velthuis, A. J.W., Worm, V.D., SH, E., Snijder, E.J., 2012. The SARS-coronavirus nsp7 + nsp8 complex is a unique multimeric RNA polymerase capable of both de novo initiation and primer extension. Nucleic Acids Res. 40 (4), 1737–1747.
Wang, J., Fang, S., Xiao, H., Chen, B., Tam, J.P., Liu, D.X., 2009. Interaction of the coronavirus infectious bronchitis virus membrane protein with beta-actin and its implication in virion assembly and budding. PloS One 4 (3), e4908.
Wang, X., Liao, Y., Yap, P.L., Png, K.J., Tam, J.P., Liu, D.X., 2009. Inhibition of protein kinase R activation and upregulation of GADD34 expression play a synergistic role in facilitating coronavirus replication by maintaining de novo protein synthesis in virus-infected cells. J. Virol. 83 (23), 12462–12472.
Xiao, Y., Ma, Q., Restle, T., Shang, W., Svergun, D.I., Ponnusamy, R., et al., 2012. Non-structural proteins 7 and 8 of feline coronavirus form a 2: 1 heterotrimer that exhibits primer-independent RNA polymerase activity. J. Virol. 86 (8), 4444–4454.
Xu, H.Y., Lim, K.P., Shen, S., Liu, D.X., 2001. Further identification and characterization of novel intermediate and mature cleavage products released from the ORF 1b region of the avian coronavirus infectious bronchitis virus 1a/1b polyprotein. Virology 288 (2), 212–222.
Xu, L., Khadijah, S., Fang, S., Wang, L., Tay, F.P.L., Liu, D.X., 2010. The cellular RNA helicase DDX1 interacts with coronavirus non-structural protein 14 and enhances viral replication. J. Virol. 84 (17), 8571–8583.
Zhai, Y., Sun, F., Li, X., Pang, H., Xu, X., Bartlam, M., et al., 2005. Insights into SARS-CoV transcription and replication from the structure of the nsp7–nsp8 hexadecamer. Nat. Struct. Mol. Biol. 12 (11), 980–986.
Zhao, X., Shaw, K., Cavanagh, D., 1993. Presence of subgenomic mRNAs in virions of coronavirus IBV. Virology 196 (1), 172–178.